Organic Electrochemical Transistor with Molecularly Imprinted Polymer Modified Gate for the Real-Time Selective Detection of Dopamine

Kan Tang,[a] Chyanne Turner,[b] Leah Case,[a] Amin Mehrehjedy,[a] Xuyang He,[c] Wujian Miao,[a] Song Guo[,a]*

a. Department of Chemistry and Biochemistry, The University of Southern Mississippi, Hattiesburg, Mississippi 39406, United States.

b. Chemistry Department, St. Lawrence University, Canton, New York, 13617, United States.

c. School of Criminal Justice, Forensic Science, and Security, The University of Southern Mississippi, Hattiesburg, Mississippi 39406, United States

* Email: song.guo@usm.edu

ABSTRACT: Due to their low operation voltage, high transconductance, and good aqueous compatibility, organic electrochemical transistors (OECTs) have been widely applied in the sensing of small redox-active molecules such as dopamine. However, selective detection of dopamine (DA) can be challenging since its sensing mechanism relies on the gate voltage offset caused by the redox chemistry at the gate electrode. To introduce selectivity towards dopamine detection, a polypyrrole film was electrochemically deposited on the Pt gate electrode with the presence of dopamine as a template and then overoxidized in an alkaline solution. The resultant

OECT sensor with an overoxidized MIP (o-MIP/Pt) gate shows a similar detection limit of ~34 nM as compared to the device with a bare Pt gate. At the same time, when compared to the drain current response of a representative interferent, ascorbate (AA), a good selectivity of DA/AA signal ratio of larger than 5 can be achieved in the concentration range between ~0.4 μM and ~10 μM, whereas OECT sensor with bare Pt gate shows little selectivity towards DA. The selectivity of the OECT sensor towards DA can be maintained in the co-presence of 1-fold DA (~0.4 μM) and 10-fold AA (~4 μM), regardless of the order of the additions.

KEYWORDS: OECT sensor, dopamine, real-time measurement, molecularly imprinted polymer, polypyrrole, overoxidation

Introduction

Organic electrochemical transistors (OECTs) with polymeric mixed conductors as the active channel have attracted increasing research interest as intriguing candidates for the applications of bioelectronics.[1-4] For example, PEDOT:PSS, as a classic benchmark p-type mixed conductor, carries both electronic charge carrier (holes) and ions in an aqueous environment, providing a great platform for the interplay of electronic and ionic conductivities.[5-8] The electronic conductivity of intrinsically doped PEDOT:PSS can be controlled by the ion injection into the active channel by applying different gate voltages. A partial dedoped state can be reached by injecting cations into the film by a positive gate bias, and the film can be redoped by a negative gate bias. In another word, the modulation of the drain current within the active channel can be tuned by the gate bias under the aqueous environment. This unique compatibility with water along with other features such as low operating voltage (sub-1 V) and high transconductance, makes it ideal to use OECT

for the sensing of various analytes in aqueous solutions such as metabolites,[9-13] neurotransmitters,[14-17] and proteins.[18-22]

Despite the working principle of the OECT sensor for a variety of analytes stems from the same idea of tracing drain current change due to the change of ion injection upon the addition of an analyte, there are multiple routes available for the realization of the OECT sensor. To the best of our knowledge, three are three major sensing mechanisms: (1) Establish a redox reaction on the surface of a metal gate electrode by maintaining a high enough bias at the gate electrode.[9, 13] The resulting redox current produced can shift the initial gate bias V_g into an effective gate bias $V_{g,\,eff}$, therefore, the active channel experiences a different gate bias, and the drain current shifts. This mechanism is widely used for the sensing of small molecules such as metabolites and neurotransmitters. [9-17] (2) Utilize the capacitance change of the gate electrode due to the binding events between antigen and antibody or commentary DNA strands.[20, 21] Typically, antibody or DNA molecules can be immobilized on the gate electrode. Once their counterparts, the analyte, bind with the modified gate surface, it induces a capacitive coupling between the biorecognition units and the active channel, resulting in a change of drain current. (3) Control the ion flow into the active channel by adding an ion channel that potentially impedes ion transport.[23-26] For example, Malliaras's group used cells with tight junctions or bilayer lipid membrane to limit the ion transport through the layer.[23, 24] More recently, Inal's group applied an amyloid-β (Aβ) selective isoporous membrane on top of the active channel that blocked the ion penetration upon binding of the Aβ protein onto the membrane.[12, 22]

Dopamine (DA) is a critical neurotransmitter in the central nervous system, its complex pathways have a significant role in the determination of reward-motivated behaviors.[27] The abnormality of dopamine level can be associated with various neurological disorders such as

Parkinson's disease,[28, 29] ADHD,[30, 31] and schizophrenia.[32, 33] Previously, Yan's group worked extensively on the highly sensitive OECT devices for the detection of dopamine based on the redox reaction at the gate electrode as mentioned in the mechanism (1) above.[11, 16] The detection limit of the OECT sensor to dopamine can be as low as 5 nM (~1 ppb) under optimal conditions. They have also shown that the modification of the gate electrode by certain materials such as anionic Nafion and graphene can greatly enhance the selectivity of the device towards dopamine versus other interferents such as ascorbate (AA), uric acid (UA), etc.[16, 34] It is worthwhile to mention that ascorbate/Vitamin C is of particular relevance as an interferent since it serves multiple roles in the brain such as a co-factor of dopamine β-hydroxylase for converting dopamine into noradrenaline, as well as a regulator of dopamine and other neurotransmitters released from the synaptic vesicles.[35]

The strategy of decorating the working electrode with anionic materials such as Nafion was devised earlier in the fast-scan voltammetry based on carbon fiber microelectrode for the selective detection of dopamine by Wightman's group.[36, 37] The idea of introducing a negatively charged surface is to promote the accumulation of cationic analytes like dopamine and reject other anionic interferents.[36-38] Using a similar principle, later on, overoxidized polypyrrole conductive film was deposited on the electrode as an anion barrier to enhance the selectivity.[39-41] To further increase the selectivity of the deposited film on the electrode, Lakshmi *et al.* proposed a bilayer structure of molecularly imprinted polymer (MIP)/conducive polymeric film on the electrode. The concept was to utilize the recognition ability of MIP and transduce the binding events of catecholamines into an electrochemical response with the help of conductive polymeric film.[42] Numerous reports on the conductive polypyrrole-based MIP for the selective detection of dopamine can be found, where the cavities were templated by dopamine during the electrochemical polymerization.[43-47]

Recently, Zhang et al. have demonstrated the idea of using OECTs with MIP modified gate for the selective detection of amino acids and ascorbic acid.[48, 49] OECTs can be operated with large currents up to several hundred μA, which is much higher than those electrochemical methods using microelectrode (nA to μA). This means OECT devices can potentially provide a better signal-to-noise ratio. So far there have been no reports on utilizing dopamine templated MIP as the gate electrode in an OECT device for the highly selective detection of dopamine. Herein, the OECT devices based on prefabricated interdigitated electrodes were used to investigate the performance of the dopamine sensor such as sensitivity and selectivity. For the o-MIP gated sensor, a detection limit of 34 nM can be achieved with a wide detection range from nM to μM. Good selectivity of the devices towards dopamine with a signal ratio of DA/AA > 5 in a concentration range between 0.35 μM and 8.8 μM can be observed from the results of the real-time experiments with separated DA and AA tests. When 1-fold DA (~0.4 μM) and 10-fold AA (~4 μM) are co-presented, similar selectivity towards DA is maintained. The results here show the effectiveness of the MIP concept in the modification of the gate electrode of the OECT device for the selective detection of dopamine, an important neurotransmitter, via the transducing of dopamine oxidation at the gate electrode.

Experimental Section

Materials. PEDOT:PSS (1.3 wt%) and (3-glycidyloxypropyl)trimethoxysilane (GOPS) were purchased from Sigma-Aldrich. Dopamine hydrochloride and ascorbic acid were purchased from Fisher Scientific. Pyrrole was from Oakwood Chemical, SC, USA. DI water was obtained from a Millipore water purification system. Electrolytes such as disodium phosphate (Na_2HPO_4), monosodium phosphate (NaH_2PO_4) were also purchased from Sigma-Aldrich. The concentrations of Na_2HPO_4 and NaH_2PO_4 were 10 mM and 1.8 mM, respectively, for the preparation of a PBS

buffer solution (pH = 7.4). Platinum plate electrodes (1 cm × 1 cm × 0.1 mm) were from Newvision, Huizhou, China. Prefabricated interdigitated electrodes (IDEs) were from NanoSPR, LLC, IL, USA. The channel length *L* of the IDEs is 20 μm, and the total channel width *W* is 20 mm (1 mm each × 20 pairs). A two-component epoxy, EPO-TEK® H70E, was purchased from Ted Pella. Gold on silicon substrates (Au/Si) with a titanium adhesion layer were purchased from Platypus Technologies, WI, USA.

Electrochemical Synthesis of the Molecular Imprinted Polymer (MIP). The insulation of Pt electrodes was reinforced by applying pre-mixed epoxy (EPO-TEK® H70E) to the junction between the Pt plate and the PTFE rod. The epoxy was cured at 100 ^{o}C for 1.5 h. Electrochemical experiments were carried out in a CHI 660A electrochemical workstation (CH Instruments, TX, USA). A conventional three-electrode system was adopted, where a Pt mesh was the counter electrode and an Ag/AgCl was used as the reference electrode. Pt plate electrode or Au/Si substrate can be used as the working electrode. Before the electrochemical deposition of polypyrrole MIP on the Pt electrodes or Au/Si substrate, the surface of the metal was cleaned in 0.5 M NaOH after five cycles of potential sweeps from -1V to +1 V with a scan rate of 100 mV/s. After rinsing the surface with DI water, three cycles of scans from 0 V to +1 V were performed in a solution of 10 mM pyrrole and 0.1 M NaCl with a scan rate of 10 mV/s. For the preparation of MIP involved Pt electrodes, 1 mM of dopamine was also presented in the deposition solution. After the deposition of polypyrrole MIP, the dopamine template was removed by dipping in ethanol for 1 h. Afterward, the MIP/Pt electrode can be further overoxidized by performing five cycles of scan from 0 to 0.5 V in 0.5 M NaOH with a scan rate of 10 mV/s. The polypyrrole-modified electrodes were stored in DI water before usage. The SEM measurements were conducted in a Zeiss Sigma VP FEG-SEM with a Thermo Scientific UltraDry EDS detector.

OECT Device Fabrication and Characterization. The fabrication method of OECTs on interdigitated electrodes followed the reported procedures.[50-52] After spin-coating PEDOT:PSS on the IDE substrate, excess PEDOT:PSS outside of the IDE region was removed by Q-tips soaked with DI water. The substrate was annealed at 140 ^{o}C for 1 h on a hotplate. After annealing, the PEDOT:PSS-free region was insulated from water contact (Sally Hansen, Insta-Dri). Transfer characteristics and real-time drain current measurements of the OECT devices were measured in a dual-channel Keithley 2612B source measure unit that was controlled by Keithley ACS software. The experiments were carried out in a glass vial with 20 mL PBS buffer (pH = 7.4). The PBS buffer in the glass vial was deaerated with high-purity N_2 for 10 min before any measurement. A steady N_2 flow was maintained on top of the solution during the experiments. The PEDOT:PSS covered IDE region of the OECT was immersed in water during all of the measurements. Pt electrode or polypyrrole modified Pt electrode was used as the gate electrode for OECTs. In transfer curve measurements, gate voltage V_g swept from 0 to +1 V while maintaining a constant drain-source voltage V_{ds} at -0.1 V. During the real-time drain current measurements, V_g was kept at +0.5 V while V_{ds} was maintained at -0.1 V. The drain current was monitored during additions of dopamine with different concentrations. The standard deviation of the baseline from the beginning trace of the plot and use it as our baseline noise. After each addition, if the current change is larger than three times of the baseline noise, the detection limit is accepted.

Results and discussion

The procedure of electrochemical synthesis of overoxidized MIP (o-MIP) is shown in Figure 1a. First, the polymerization of pyrrole on Pt electrode was carried out in a mixture solution of dopamine template and pyrrole monomer. A 1:10 molar ratio between DA template (1 mM) and pyrrole (10 mM) was adopted as suggested by the previous report to achieve optimal selectivity

towards DA.[45] After three cycles of deposition were employed, a dark brown film was formed on the surface of the electrode (Figure S1a and S1c). The oxidation peaks of dopamine and pyrrole monomer are around 0.55 V and 0.9 V (Figure 1c), respectively. The dopamine peak is only presented in the first scan cycle, in which the oxidation peak of pyrrole shows a gradual increase of magnitude, which indicates the conductive nature of the MIP film as well as the gradual increase of film thickness. After the removal of the template by ethanol wash, the polypyrrole MIP was further oxidized in 0.5 M NaOH to enhance its selectivity by introducing more hydrophilic groups into the MIP film.[40, 45] The color of the overoxidized film turned almost transparent after this step (Figure S1b and S1e). The overoxidation of MIP mainly occurs in the first scan cycle with a major oxidation peak at around 0.35 V (Figure 1d). The SEM image of pristine polypyrrole film (Figure 1e) exhibits a uniform morphology, possibly due to the regular and compact growth of MIP under a slow scan rate (10 mV/s) during the deposition. While after overoxidation, the dendritic-like feature can be observed on the surface of MIP film (Figure 1f), which can be attributed to the etching from the electrochemical oxidation in the alkaline environment, which is consistent with the previous report on the morphology of overoxidized polypyrrole.[53] The FTIR spectrum of pristine MIP polypyrrole film in Figure S2 shows peaks at ~3400 cm^{-1}, ~1500 cm^{-1}, and ~1400 cm^{-1}, that can be assigned to the stretching mode of N-H, C-C, and C-N, respectively, which confirm the successful deposition of polypyrrole on the electrode.[53-55] The peaks at ~3000 cm^{-1} and ~1000 cm^{-1} are typically attributed to the stretching of the C-H bond.[44, 56]

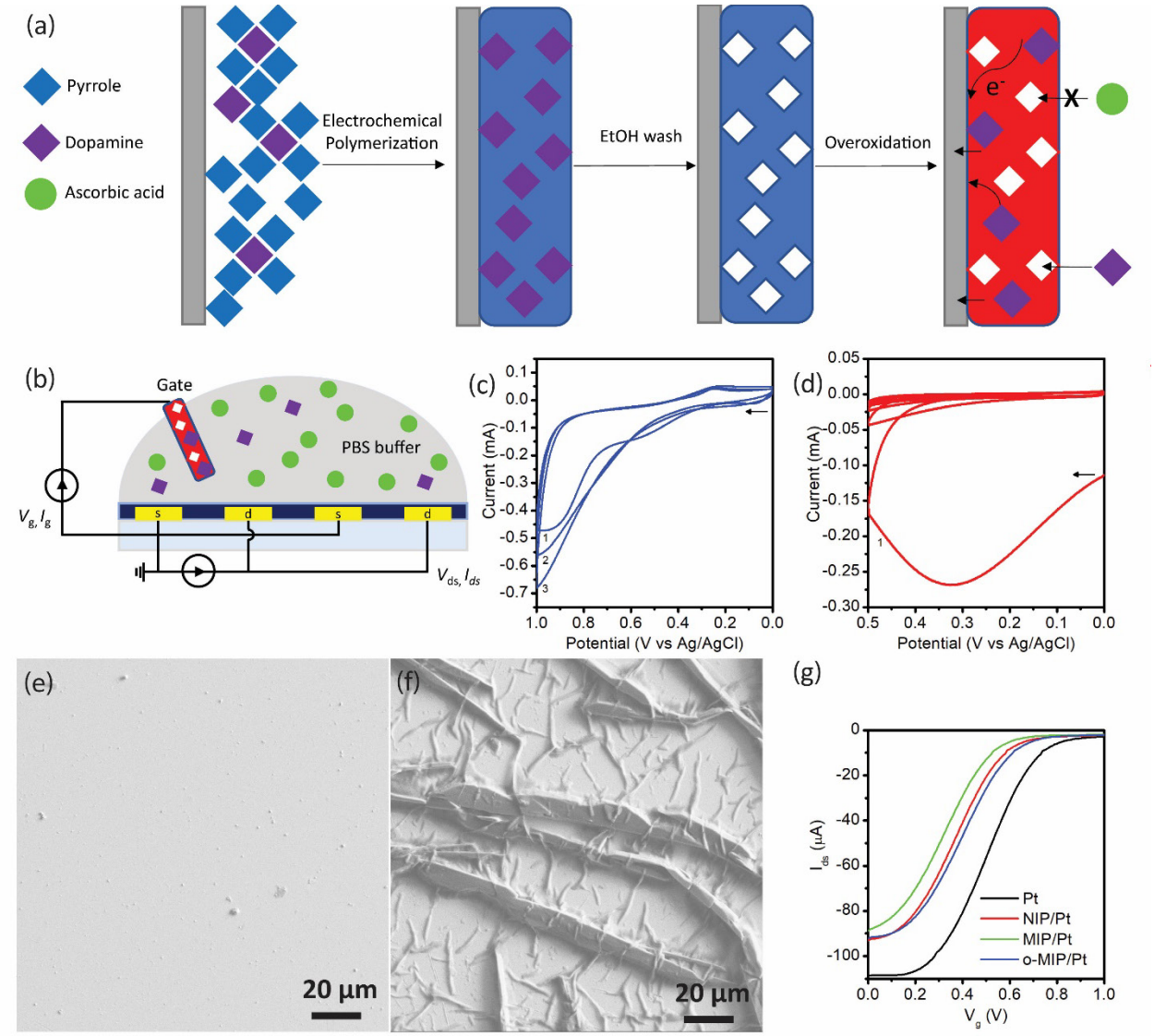

Figure 1. (a) Electrochemical synthesis of dopamine-specific o-MIP on Pt electrode. Pyrrole monomer was first deposited on Pt via electrochemical polymerization. After the removal of the dopamine template by ethanol wash, the MIP was further oxidized in 0.5 M NaOH. (b) Schematic representation of the OECT sensor with overoxidized dopamine-specific MIP as the gate electrode. (c) Cyclic voltammogram of the pyrrole (10 mM) polymerization with the presence of dopamine template (1 mM) on Pt electrode. Three cycles of deposition were deployed in 0.1 M NaCl. The scan rate is 10 mV/s. The arrow in the panel indicates the starting point and the direction of the potential scan. (d) Cyclic voltammogram of the overoxidation of polypyrrole MIP in 0.5 M NaOH.

Five cycles were applied in the oxidation process. The scan rate is 10 mV/s. The arrow in the panel indicates the starting point and the direction of the potential scan. (e) SEM image of pristine polypyrrole MIP on Au/Si substrate. (f) SEM image of overoxidized polypyrrole MIP on Au/Si substrate. (g) Transfer curves of OECT device with bare Pt, NIP, MIP, and overoxidized MIP on Pt as the gate electrode.

The MIP-modified Pt electrode is adopted as the gate of an OECT device for the selective detection of DA (Figure 1b). As mentioned before, the sensing mechanism based on the redox chemistry at the gate electrode requires appropriate gate biases to ensure the conversion of the analyte added. Here, a positive bias is needed for the oxidative conversion of dopamine into *o*-dopaminequinone to proceed on the gate electrode. Although a higher gate bias promotes the conversion of dopamine at the gate electrode, it needs to be compromised with the transconductance (g_m). As maximal g_m is typically achieved below +0.5 V for the PEDOT:PSS based OECTs,[57] the gate voltage (V_g) applied should not be too high so that the device becomes insensitive to the oxidation reaction at the gate electrode due to the severe suppression of g_m. Meanwhile, a higher gate bias is not favored for the device stability of OECTs.[52, 58] Yan's group has shown that a gate bias of 0.4 to 0.6 V might be an ideal range of gate bias for the OECT sensor targeted at dopamine.[17] Therefore, the OECT devices in this report are operated in their "off" state with V_g maintained at +0.5 V during the measurement to assure a balance of selectivity, sensitivity, and stability for the o-MIP gate electrode. To verify whether this gate bias condition is ideal for the applications of various polypyrrole-modified gate electrodes, their transfer characteristics were investigated. In Figure 1g, the transfer curves of OECTs with bare Pt, non-imprinted polymer on Pt (NIP/Pt), MIP/Pt, and o-MIP/Pt, as the gate electrode are presented. The transfer curve shifts significantly to the lower voltage side of the Pt curve when the gate electrode is coated with a layer

of conductive polypyrrole, where the MIP/Pt gate shifts the most while o-MIP/Pt shifts the least. The transfer curve difference between NIP/Pt and MIP/Pt is likely due to the presence of dopamine during the preparation of MIP could lead to a different morphology and chemical composition of the MIP film from the NIP film, which can result in different capacitances. The interplay between the capacitances of the channel/electrolyte interface (C_C) and the gate/electrolyte interface (C_G) determines the charge distribution between gate/ electrolyte and electrolyte/channel when a gate voltage is applied, and therefore determines the current in the active channel. Thus, the $V_{g,\,m}$ associated with the maximal g_m values also varies when different gate electrodes are used (Figure S3). The $V_{g,\,m}$ values of the Pt gate is about +0.5 V, which is very close to the ideal oxidation potential needed for the oxidative detection of dopamine. In contrast, MIP/Pt shows a lower $V_{g,\,m}$ at about +0.3 V, implying a reduced sensitivity when +0.5 V is applied for the oxidation of dopamine. o-MIP/Pt shows a recovered $V_{g,\,m}$ at about +0.4 V, which suggests that it might have a better sensitivity as compared to MIP/Pt in the detection of dopamine.

In Figure 2a, the real-time evolution of the drain current (I_{ds}) of the OECT sensor with bare Pt gate upon consecutive additions of DA is shown. Under constant bias conditions (V_g = +0.5 V, V_{ds} = -0.1 V), the first two additions introduce little change to the I_{ds}. When a third addition of the DA (26 nM or 5 ppb) is implemented, the trace of I_{ds} deviates from the baseline and levels off after ~100s, exhibiting a staircase-like change of the signal. This staircase signal has been widely reported in the detections of neurotransmitters and metabolites,[15, 16, 34, 44] and in general, it can be regarded as a characteristic feature of the successful detection of the analyte using redox chemistry at the gate electrode. This type of current decrease can be observed at every DA addition above 26 nM, resulting in an ascending series of staircases towards lower absolute values of I_{ds}. The size of the decrement of I_{ds} upon each addition first increases from the 3rd to 7th addition (2.6 μM) and

then decreases after that. Finally, the 10th addition (53 μM) of the DA results in a negligible change of I_{ds}, indicating the saturation of the device and the range of measurement in DA sensing. For the AA detection, OECT with bare Pt appears to respond to even lower concentrations as the staircase shift of the I_{ds} can be observed at the first addition (Figure 2b). Similar to the DA detection, the upward shift of I_{ds} can be traced upon the additions of AA with increasing concentrations. The saturation of the I_{ds} is not seen for the AA detection using Pt gated OECT, however, the 10th addition indeed results in reduced size of the step, which matches the general trend observed in the second stage (8th to 10th as shown in Figure 2a) of DA detection using Pt gated OECT. These reduced step sizes indicate that the device will eventually saturate at very high analyte concertation.

The behaviors of Pt gated OECT for both DA and AA sensing are summarized in Figure 2c by plotting the normalized ending current response (NCR) of each step as a function of accumulated analyte concentrations. The definition of NCR can be expressed as follows,[11, 17]

$$NCR = \left|\frac{I_{ds} - I_{ds,0}}{I_{ds,0}}\right| \quad (1)$$

where I_{ds} is the ending current of the step upon each addition of analyte, $I_{ds,0}$ is the drain current before the addition of an analyte. Both curves are *S*-shaped as the slopes at low concentration regime (<0.1 μM) and high concentration regime (>10 μM) are much smaller than that at the intermediate concentration regime (0.1 to 10 μM) where the highest sensitivity (dI/dc) is achieved.[15, 59] The NCR response of AA is higher than that of DA when the analyte concentration is lower than 0.1 μM. However, Pt gated OECT has a higher sensitivity in DA as indicated by the larger slope as compared to AA sensing at above 0.1 μM. This also explains the previous observation that the detection of DA reaches NCR saturation quicker than the detection of AA. At

the accumulative concentration of 88 μM after the 10th addition, the ending NCR value of the DA sensor is ~0.9, while the AA sensor has a slightly lower ending NCR value of ~0.8.

Although Pt gated OECT sensor has slight differences in detection limit, range of measurement, and sensitivity, the NCR curves of DA and AA as a function of concentration still generally overlay each other. Therefore, it is difficult to differentiate DA as an analyte in case AA is presented as an interferent in a similar quantity or even in large excess. As mentioned before, the dopamine-targeted MIP can provide a better selectivity of the OECT sensor towards DA detection. However, the MIP/Pt gate OECT sensor is not very sensitive to dopamine. As shown in Figure S4a, at the low concentration regime, the I_{ds} shifts downwards upon the addition of DA, which is not the typical staircase signal ascribed to the oxidation of dopamine. It only shows a noticeable well-defined step-like change of the I_{ds} after the accumulative concentration of dopamine exceeds 0.35 μM, which is about 10 times higher in comparison with the detection limit of Pt gated devices. A similar observation is made in the NIP/Pt gated sensor (Figure S4b), which could result from a combination of the lack of dopamine-specific cavities and a shift in the transfer characteristics. The similar DA sensitivities between MIP/Pt and NIP/Pt imply that the advantage of introducing MIP cavities specific for DA along is not enough to overcome the negative impact caused by the shift of transfer characteristics. Additionally, in the MIP/Pt and NIP/Pt cases, there seem to be some separate mechanisms besides the oxidation of dopamine, which results in the changes of I_{ds} in the opposite direction of the step-like ones. This phenomenon is more evident when the concentration of dopamine is low, where the contribution from oxidation current is not dominant. Further investigation is needed to elucidate this question.

In Figure 2d, a real-time trace of o-MIP/Pt gated OECT for the sensing of DA is presented. The overall response resembles the Pt gated OECT. The first noticeable step-like shift is observed at

the 3rd addition (26 nM or 5 ppb). Afterward, an ascending pattern of the step-like signal can be established upon consecutive additions of DA. The I_{ds} also saturates at the 10th addition. On the other hand, o-MIP/Pt gated OECT shows a drastically different response in AA sensing as compared to Pt gated sensor (Figure 2e). No well-defined staircase signal can be observed from the 1st to the 3rd addition, and the current starts to trend slightly downward from the 3rd addition. Within the first eight additions, the step-like change of I_{ds} is greatly suppressed. However, after the accumulative concentration reaches above 10 μM, a dramatic step can be observed at the 9th addition of DA, which indicates that at that stage MIP is not effective anymore in the blocking of AA oxidation. This indicates the upper concentration limit of the selectivity of o-MIP. It is possible that when AA concentration reaches above a certain threshold value, i.e. 10 μM, oxidation of AA can occur on the surface of MIP film without binding with the selective cavities within the MIP film.

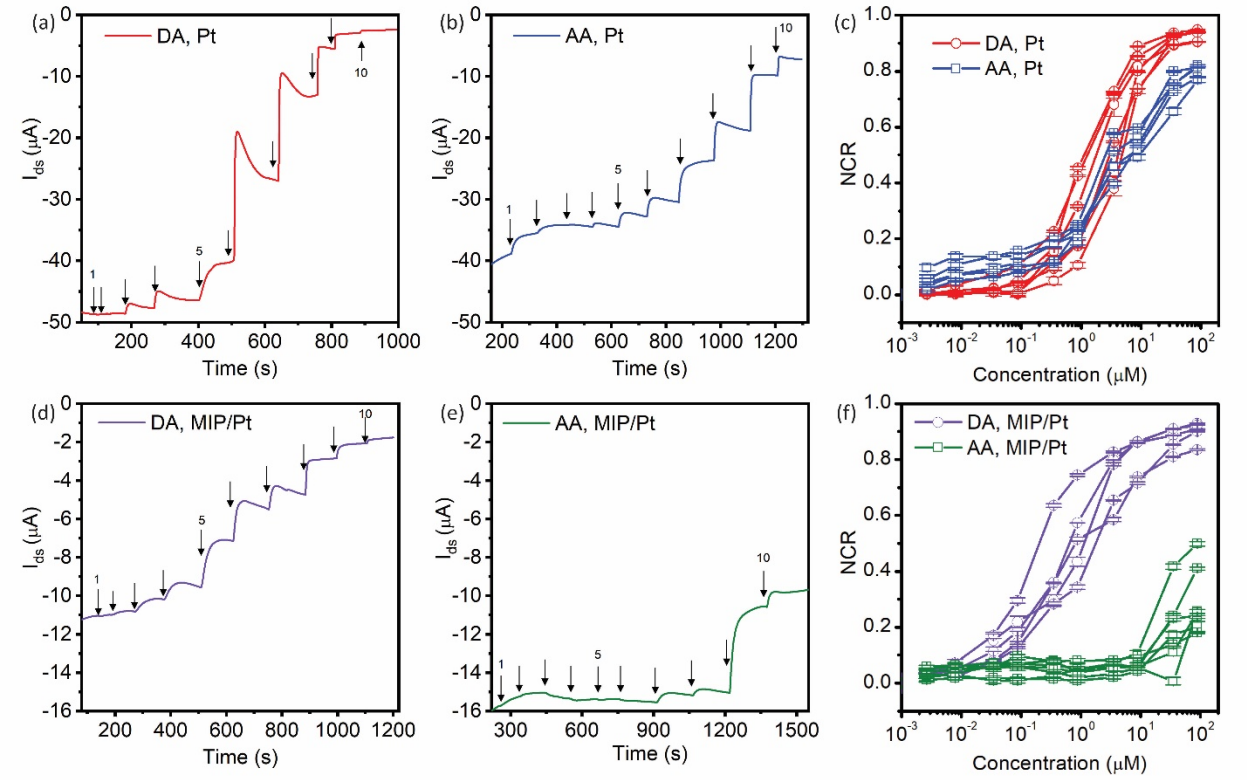

Figure 2. (a, b) Real-time trace of drain current I_{ds} of OECT sensors with Pt gate upon sequential additions of dopamine (a) and ascorbate (b) in PBS buffer. (c) Normalized current response (NCR) of OECT sensors with Pt gate as a function of added analyte concentrations. (d, e) Real-time trace of drain current I_{ds} of OECT sensor with MIP/Pt gate upon sequential additions of dopamine (d) and ascorbate (e) in PBS buffer. (f) Normalized current response (NCR) of OECT sensors with MIP/Pt gate as a function of added analyte concentrations. Vg = +0.5 V, V_{ds} = -0.1 V. The concentrations of 10 consecutive additions of the analyte are 2.6 nM, 5.3 nM, 26 nM, 53 nM, 0.26 μM, 0.53 μM, 2.6 μM, 5.3 μM, 26 μM, and 53 μM. The first, 5^{th}, and 10^{th} additions of the analyte are labeled for eye guidance. Every real-time experiment was reproduced in 5 devices.

The NCR of o-MIP/Pt gated OECT can be referred to in Figure 2f. It is clear to observe the separation of two curves when the accumulative concentration exceeds 0.1 μM. NCR of DA sensing with o-MIP/Pt exhibits "S-shaped" characteristics similar to that with Pt gated sensor, which presents the highest sensitivity in the intermediate range of accumulative concentration between 0.1 μM and 10 μM. The final NCR value of MIP/Pt gated OECT is about 0.9, which is also close to the bare Pt gated OECT. In contrast, the AA sensor shows no significant sensitivity until an accumulative concentration of 10 μM. Due to the direct oxidation of AA on the surface of the film at high concentration, the NCR of the AA sensor sharply increases at above 10 μM. However, even with the abrupt increase, the ending NCR value is still lower than that in the DA sensor, which implies that the selectivity of MIP still partially remains at an accumulative concentration of 88 μM. Therefore, it would be interesting to compare the performance between Pt gated and o-MIP/Pt gated OECTs in terms of selective detection of DA under different concentration regimes.The normalized current response of OECTs with or without the o-MIP layer

on the Pt gate electrode at three representative concentrations is shown in Figure 3. As for the bare Pt gate electrode, the NCR values from dopamine and ascorbate are indistinguishable at the intermediate regime of the accumulative analyte concentration (0.35 μM). When entering into a higher accumulative concentration regime (i.e. > 8 μM), NCR values from DA become larger than those from AA, which indicates a slight selectivity towards dopamine. However, this intrinsic selectivity only works at relatively high analyte concentrations. Throughout the concentration range, the best selectivity ratio of NCR_{DA}/NCR_{AA} is still below 1.6 for Pt gated OECT. On the other hand, the MIP coated Pt electrode shows better selectivity towards dopamine at all representative concentrations as compared to bare Pt. The NCR_{DA}/NCR_{AA} ratio is ~ 7.6 at 0.35 μM and ~13 at 8.8 μM. As for the high concentration at 88 μM, the selectivity of the OECT sensor decreases to about 3. This is consistent with the observation of the abrupt increment of NCR signal in Figure 2f when AA concentration exceeds 10 μM, indicating the reduction of the effectiveness of MIP in the suppression of parasitic contribution to the gate voltage offset from AA oxidation.

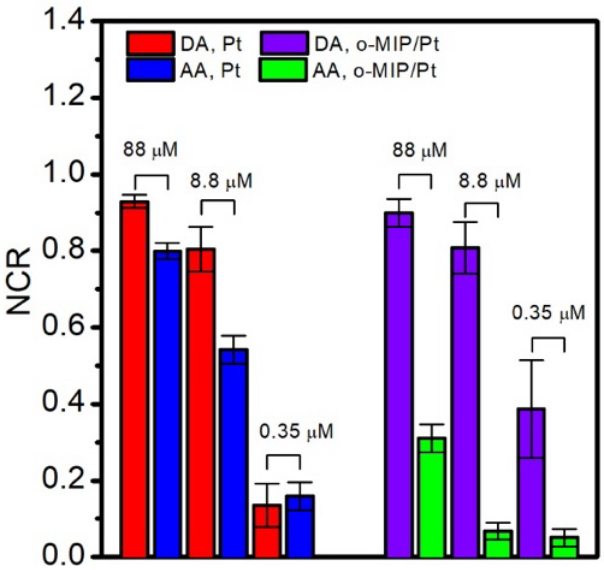

Figure 3. Normalized current response (NCR) of OECT sensors with Pt gate or o-MIP/Pt gate at different accumulative analyte concentrations. Note that the MIP is templated by dopamine. DA

stands for dopamine and AA stands for ascorbate. Each error bar is derived from the NCR of 5 devices.

Since o-MIP/Pt exhibits a good selectivity towards DA in an accumulative intermediate concentration of ~0.4 μM, it is also valuable to investigate its selectivity with the presence of a large excess of interferent such as AA. The introduction of a large excess interferent (i.e. 10-fold) is a typical method to verify if the parasitic contribution from the interferent is involved, which provides a straightforward way to examine the selectivity of an electrochemical sensor. As shown in Figure 4a, a drastic step of I_{ds} can be observed after the addition of ~0.4 μM DA, which is followed by an insignificant change of the signal after the addition of 10-fold AA (4 μM). When the order of additions is swapped, a small step shift upwards caused by the addition of 10-fold AA is first observed, and then after the introduction of DA, a major step signal can be produced (Figure 4b). These observations not only show an insignificant interference of the signal caused by the introduction of 10-fold AA, at the same time, they also illustrate that the appearance of a DA step signal is not dependent on the order of the additions. This result shows that DA dominantly occupies the cavities in the MIP layer while AA is not strongly adsorbed within the MIP film.

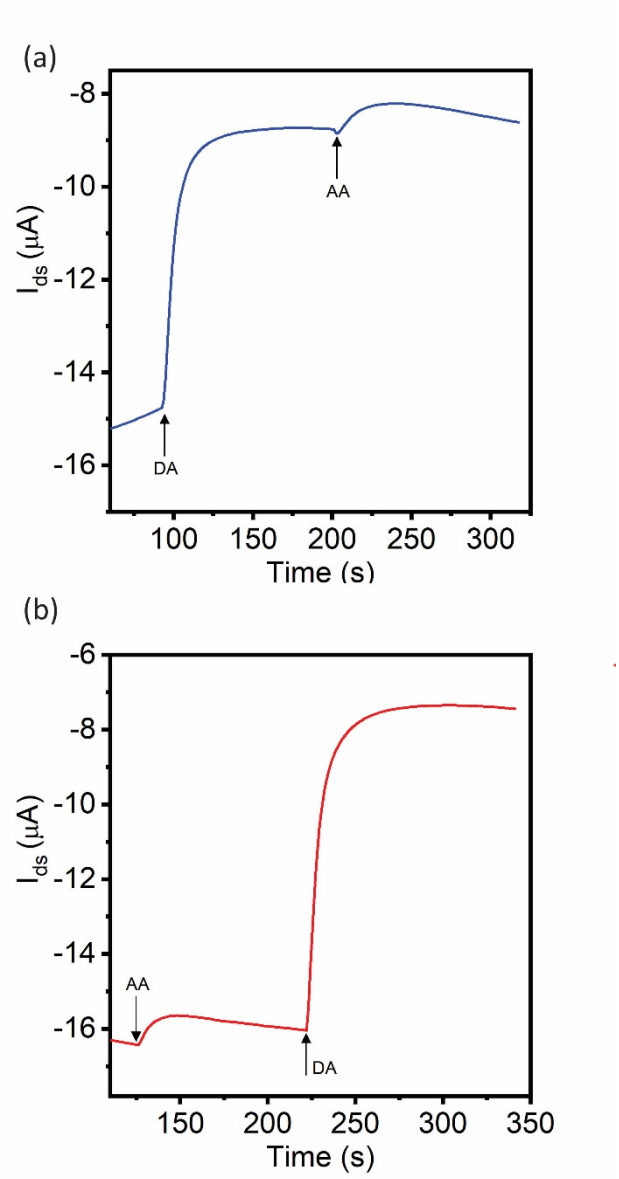

Figure 4. Real-time trace of I_{ds} of OECT sensor with o-MIP/Pt gate upon alternating additions of DA (0.4 μM) and 10-fold interferent AA (4 μM) in PBS buffer. (a) First DA then AA. (b) First AA then DA. V_g = +0.5 V, V_{ds} = -0.1 V.

Conclusions

In conclusion, this work has devised a facile approach for the preparation of dopamine selective OECT sensor based on MIP modified gate electrode. A series of polypyrrole-derived films on Pt

can be electrochemical synthesized, including NIP, MIP, and o-MIP. The transfer characteristics of MIP/Pt gated OECT deviate the most from the reference curve of the bare Pt gated device with a $V_{g,\,m}$ associated with maximal transconductance at about +0.3 V, which intrinsically disfavors the oxidation of dopamine. Both MIP/Pt and NIP/Pt gated sensors have a rather high DA detection limit at ~0.35 μM, which is not as good as the Pt gated device (~34 nM or 6.5 ppb). Despite good sensitivity and low detection, the Pt gate electrode shows little DA selectivity in the drain current response when compared with the results from AA in the same concentration range (0.1 to 100 μM). o-MIP/Pt, showing good $V_{g,\,m,}$ with specific cavities for DA, exhibits good sensitivity and selectivity in the DA detection. Furthermore, the o-MIP gated sensor achieved a similar detection limit as compared to the Pt gated device, largely because its $V_{g,\,m}$ align with the ideal oxidation potential for DA. Meanwhile, a good selectivity of DA/AA signal ratio of larger than 5 can be achieved in the concentration range between ~0.4 μM and ~10 μM. The performance of the OECT sensor gated with o-MIP/Pt can be maintained in the co-presence of 1-fold of DA analyte and 10-fold of AA interferent. With the merits of low cost and convenience by electrochemical deposition, molecularly imprinted polymers (MIPs) offer promising possibilities for the fabrication of highly selective OECT sensors, without the presence of high-specific yet expensive surface modifiers such as enzymes and antibodies. We hope the concept of this work on the real-time selective detection of dopamine based on MIP gated OECT can be further expanded into the sensing of other redox-active small molecules or neurotransmitters.

ASSOCIATED CONTENT

Supporting Information. The following files are available free of charge at https://pubs.acs.org

Additional figures including images of MIP electrodes, FT-IR spectra, transconductance plots, real-time drain current of OECT as discussed in the main text (PDF).

AUTHOR INFORMATION

Corresponding Author

* Song Guo − Department of Chemistry and Biochemistry, University of Southern Mississippi, Hattiesburg, Mississippi 39406, United States; orcid.org/0000-0002-3457-4331; Email: song.guo@usm.edu; Phone: (+1)601-266-4702

Author Contributions

K.T., X.H., W.M. and S.G. conceived the idea. K.T., C.T., L.C., A.M., and X.H. prepared the OECT devices and conducted the OECT measurements. K.T. conducted the CV measurements. X.H. conducted the FT-IR measurements. K.T., C.T., X.H., W.M. and S.G. analyzed the data. K.T. and S.G. wrote the manuscript with contribution of all authors. All authors have approved the final version of the manuscript.

Notes

The authors declare no competing financial interest

ACKNOWLEDGMENT

This work was supported by a National Science Foundation under grant number 1554841 and 1757220. C.T. acknowledg-es the support from NSF-CHE-1950840. Authors would like to thank Michael Blanton for his help in SEM measurements.

REFERENCES

1. Chen, S.; Surendran, A.; Wu, X.; Lee, S. Y.; Stephen, M.; Leong, W. L., Recent Technological Advances in Fabrication and Application of Organic Electrochemical Transistors. *Adv. Mater. Technol.* **2020,** *5* (12), 2000523.
2. Moser, M.; Ponder Jr, J. F.; Wadsworth, A.; Giovannitti, A.; McCulloch, I., Materials in organic electrochemical transistors for bioelectronic applications: past, present, and future. *Adv. Funct. Mater.* **2019,** *29* (21), 1807033.
3. Paulsen, B. D.; Tybrandt, K.; Stavrinidou, E.; Rivnay, J., Organic mixed ionic–electronic conductors. *Nat. Mater.* **2020,** *19* (1), 13-26.

4. Rivnay, J.; Inal, S.; Salleo, A.; Owens, R. M.; Berggren, M.; Malliaras, G. G., Organic electrochemical transistors. *Nat. Rev. Mater.* **2018,** *3* (2), 1-14.
5. Bernards, D. A.; Malliaras, G. G., Steady-state and transient behavior of organic electrochemical transistors. *Adv. Funct. Mater.* **2007,** *17* (17), 3538-3544.
6. Inal, S.; Malliaras, G. G.; Rivnay, J., Benchmarking organic mixed conductors for transistors. *Nat. Commun.* **2017,** *8* (1), 1-7.
7. Khodagholy, D.; Rivnay, J.; Sessolo, M.; Gurfinkel, M.; Leleux, P.; Jimison, L. H.; Stavrinidou, E.; Herve, T.; Sanaur, S.; Owens, R. M., High transconductance organic electrochemical transistors. *Nat. Commun.* **2013,** *4* (1), 1-6.
8. Rivnay, J.; Leleux, P.; Ferro, M.; Sessolo, M.; Williamson, A.; Koutsouras, D. A.; Khodagholy, D.; Ramuz, M.; Strakosas, X.; Owens, R. M., High-performance transistors for bioelectronics through tuning of channel thickness. *Sci. Adv.* **2015,** *1* (4), e1400251.
9. Bernards, D. A.; Macaya, D. J.; Nikolou, M.; DeFranco, J. A.; Takamatsu, S.; Malliaras, G. G., Enzymatic sensing with organic electrochemical transistors. *J. Mater. Chem.* **2008,** *18* (1), 116-120.
10. Liao, C.; Mak, C.; Zhang, M.; Chan, H. L.; Yan, F., Flexible organic electrochemical transistors for highly selective enzyme biosensors and used for saliva testing. *Adv. Mater.* **2015,** *27* (4), 676-681.
11. Tang, H.; Yan, F.; Lin, P.; Xu, J.; Chan, H. L., Highly sensitive glucose biosensors based on organic electrochemical transistors using platinum gate electrodes modified with enzyme and nanomaterials. *Adv. Funct. Mater.* **2011,** *21* (12), 2264-2272.
12. Wustoni, S.; Savva, A.; Sun, R.; Bihar, E.; Inal, S., Enzyme-free detection of glucose with a hybrid conductive gel electrode. *Adv. Mater. Interfaces* **2019,** *6* (1), 1800928.
13. Zhu, Z.-T.; Mabeck, J. T.; Zhu, C.; Cady, N. C.; Batt, C. A.; Malliaras, G. G., A simple poly (3, 4-ethylene dioxythiophene)/poly (styrene sulfonic acid) transistor for glucose sensing at neutral pH. *Chem. Commun.* **2004,** (13), 1556-1557.
14. Gualandi, I.; Tonelli, D.; Mariani, F.; Scavetta, E.; Marzocchi, M.; Fraboni, B., Selective detection of dopamine with an all PEDOT: PSS organic electrochemical transistor. *Sci. Rep.* **2016,** *6* (1), 1-10.
15. Kergoat, L.; Piro, B.; Simon, D. T.; Pham, M. C.; Noël, V.; Berggren, M., Detection of glutamate and acetylcholine with organic electrochemical transistors based on conducting polymer/platinum nanoparticle composites. *Adv. Mater.* **2014,** *26* (32), 5658-5664.
16. Liao, C.; Zhang, M.; Niu, L.; Zheng, Z.; Yan, F., Organic electrochemical transistors with graphene-modified gate electrodes for highly sensitive and selective dopamine sensors. *J. Mater. Chem. B* **2014,** *2* (2), 191-200.
17. Tang, H.; Lin, P.; Chan, H. L.; Yan, F., Highly sensitive dopamine biosensors based on organic electrochemical transistors. *Biosens. Bioelectron.* **2011,** *26* (11), 4559-4563.
18. Fu, Y.; Wang, N.; Yang, A.; Law, H. K. w.; Li, L.; Yan, F., Highly sensitive detection of protein biomarkers with organic electrochemical transistors. *Adv. Mater.* **2017,** *29* (41), 1703787.
19. Koklu, A.; Wustoni, S.; Musteata, V.-E.; Ohayon, D.; Moser, M.; McCulloch, I.; Nunes, S. P.; Inal, S., Microfluidic Integrated Organic Electrochemical Transistor with a Nanoporous Membrane for Amyloid-β Detection. *ACS Nano* **2021**, 8130–8141.
20. Macchia, E.; Romele, P.; Manoli, K.; Ghittorelli, M.; Magliulo, M.; Kovács-Vajna, Z. M.; Torricelli, F.; Torsi, L., Ultra-sensitive protein detection with organic electrochemical transistors printed on plastic substrates. *Flexible Printed Electron.* **2018,** *3* (3), 034002.

21. Mulla, M. Y.; Tuccori, E.; Magliulo, M.; Lattanzi, G.; Palazzo, G.; Persaud, K.; Torsi, L., Capacitance-modulated transistor detects odorant binding protein chiral interactions. *Nat. Commun.* **2015,** *6* (1), 1-9.
22. Wustoni, S.; Wang, S.; Alvarez, J. R.; Hidalgo, T. C.; Nunes, S. P.; Inal, S., An organic electrochemical transistor integrated with a molecularly selective isoporous membrane for amyloid-β detection. *Biosens. Bioelectron.* **2019,** *143*, 111561.
23. Bernards, D. A.; Malliaras, G. G.; Toombes, G. E.; Gruner, S. M., Gating of an organic transistor through a bilayer lipid membrane with ion channels. *Appl. Phys. Lett.* **2006,** *89* (5), 053505.
24. Jimison, L. H.; Tria, S. A.; Khodagholy, D.; Gurfinkel, M.; Lanzarini, E.; Hama, A.; Malliaras, G. G.; Owens, R. M., Measurement of barrier tissue integrity with an organic electrochemical transistor. *Adv. Mater.* **2012,** *24* (44), 5919-5923.
25. Yao, C.; Li, Q.; Guo, J.; Yan, F.; Hsing, I. M., Rigid and flexible organic electrochemical transistor arrays for monitoring action potentials from electrogenic cells. *Adv. Healthc. Mater.* **2015,** *4* (4), 528-533.
26. Yao, C.; Xie, C.; Lin, P.; Yan, F.; Huang, P.; Hsing, I. M., Organic electrochemical transistor array for recording transepithelial ion transport of human airway epithelial cells. *Adv. Mater.* **2013,** *25* (45), 6575-6580.
27. Berridge, K. C., The debate over dopamine's role in reward: the case for incentive salience. *Psychopharmacology* **2007,** *191* (3), 391-431.
28. Bernheimer, H.; Birkmayer, W.; Hornykiewicz, O.; Jellinger, K.; Seitelberger, F., Brain dopamine and the syndromes of Parkinson and Huntington Clinical, morphological and neurochemical correlations. *J. Neurol. Sci.* **1973,** *20* (4), 415-455.
29. Höglinger, G. U.; Rizk, P.; Muriel, M. P.; Duyckaerts, C.; Oertel, W. H.; Caille, I.; Hirsch, E. C., Dopamine depletion impairs precursor cell proliferation in Parkinson disease. *Nat. Neurosci.* **2004,** *7* (7), 726-735.
30. Swanson, J. M.; Flodman, P.; Kennedy, J.; Spence, M. A.; Moyzis, R.; Schuck, S.; Murias, M.; Moriarity, J.; Barr, C.; Smith, M., Dopamine genes and ADHD. *Neurosci. Biobehav. Rev.* **2000,** *24* (1), 21-25.
31. Volkow, N. D.; Wang, G.-J.; Kollins, S. H.; Wigal, T. L.; Newcorn, J. H.; Telang, F.; Fowler, J. S.; Zhu, W.; Logan, J.; Ma, Y., Evaluating dopamine reward pathway in ADHD: clinical implications. *JAMA* **2009,** *302* (10), 1084-1091.
32. Davis, K. L.; Kahn, R. S.; Ko, G.; Davidson, M., Dopamine in schizophrenia: a review and reconceptualization. *Am. J. Psychiatry* **1991**.
33. Seeman, P., Dopamine receptors and the dopamine hypothesis of schizophrenia. *Synapse* **1987,** *1* (2), 133-152.
34. Zhang, M.; Liao, C.; Yao, Y.; Liu, Z.; Gong, F.; Yan, F., High-Performance Dopamine Sensors Based on Whole-Graphene Solution-Gated Transistors. *Adv. Funct. Mater.* **2014,** *24* (7), 978-985.
35. Plevin, D.; Galletly, C., The neuropsychiatric effects of vitamin C deficiency: a systematic review. *BMC Psychiatry* **2020,** *20* (1), 1-9.
36. Baur, J. E.; Kristensen, E. W.; May, L. J.; Wiedemann, D. J.; Wightman, R. M., Fast-scan voltammetry of biogenic amines. *Anal. Chem.* **1988,** *60* (13), 1268-1272.
37. Wiedemann, D. J.; Basse-Tomusk, A.; Wilson, R. L.; Rebec, G. V.; Wightman, R. M., Interference by DOPAC and ascorbate during attempts to measure drug-induced changes in

neostriatal dopamine with Nafion-coated, carbon-fiber electrodes. *J. Neurosci. Methods* **1990,** *35* (1), 9-18.
38. Robinson, D. L.; Hermans, A.; Seipel, A. T.; Wightman, R. M., Monitoring rapid chemical communication in the brain. *Chem. Rev.* **2008,** *108* (7), 2554-2584.
39. Hsueh, C.; Brajter-Toth, A., Electrochemical preparation and analytical applications of ultrathin overoxidized polypyrrole films. *Anal. Chem.* **1994,** *66* (15), 2458-2464.
40. Pihel, K.; Walker, Q. D.; Wightman, R. M., Overoxidized polypyrrole-coated carbon fiber microelectrodes for dopamine measurements with fast-scan cyclic voltammetry. *Anal. Chem.* **1996,** *68* (13), 2084-2089.
41. Witkowski, A.; Brajter-Toth, A., Overoxidized polypyrrole films: a model for the design of permselective electrodes. *Anal. Chem.* **1992,** *64* (6), 635-641.
42. Lakshmi, D.; Bossi, A.; Whitcombe, M. J.; Chianella, I.; Fowler, S. A.; Subrahmanyam, S.; Piletska, E. V.; Piletsky, S. A., Electrochemical sensor for catechol and dopamine based on a catalytic molecularly imprinted polymer-conducting polymer hybrid recognition element. *Anal. Chem.* **2009,** *81* (9), 3576-3584.
43. Maouche, N.; Guergouri, M.; Gam-Derouich, S.; Jouini, M.; Nessark, B.; Chehimi, M. M., Molecularly imprinted polypyrrole films: Some key parameters for electrochemical picomolar detection of dopamine. *J. Electroanal. Chem.* **2012,** *685*, 21-27.
44. Qian, T.; Yu, C.; Zhou, X.; Ma, P.; Wu, S.; Xu, L.; Shen, J., Ultrasensitive dopamine sensor based on novel molecularly imprinted polypyrrole coated carbon nanotubes. *Biosens. Bioelectron.* **2014,** *58*, 237-241.
45. Tsai, T.-C.; Han, H.-Z.; Cheng, C.-C.; Chen, L.-C.; Chang, H.-C.; Chen, J.-J. J., Modification of platinum microelectrode with molecularly imprinted over-oxidized polypyrrole for dopamine measurement in rat striatum. *Sens. Actuators, B* **2012,** *171*, 93-101.
46. Yang, J.; Hu, Y.; Li, Y., Molecularly imprinted polymer-decorated signal on-off ratiometric electrochemical sensor for selective and robust dopamine detection. *Biosens. Bioelectron.* **2019,** *135*, 224-230.
47. Yang, Z.; Liu, X.; Wu, Y.; Zhang, C., Modification of carbon aerogel electrode with molecularly imprinted polypyrrole for electrochemical determination of dopamine. *Sens. Actuators, B* **2015,** *212*, 457-463.
48. Zhang, L.; Liu, Z.; Xiong, C.; Zheng, L.; Ding, Y.; Lu, H.; Zhang, G.; Qiu, L., Selective recognition of Histidine enantiomers using novel molecularly imprinted organic transistor sensor. *Org. Electron.* **2018,** *61*, 254-260.
49. Zhang, L.; Wang, G.; Wu, D.; Xiong, C.; Zheng, L.; Ding, Y.; Lu, H.; Zhang, G.; Qiu, L., Highly selective and sensitive sensor based on an organic electrochemical transistor for the detection of ascorbic acid. *Biosens. Bioelectron.* **2018,** *100*, 235-241.
50. Flagg, L. Q.; Bischak, C. G.; Onorato, J. W.; Rashid, R. B.; Luscombe, C. K.; Ginger, D. S., Polymer crystallinity controls water uptake in glycol side-chain polymer organic electrochemical transistors. *J. Am. Chem. Soc.* **2019,** *141* (10), 4345-4354.
51. Flagg, L. Q.; Giridharagopal, R.; Guo, J.; Ginger, D. S., Anion-dependent doping and charge transport in organic electrochemical transistors. *Chem. Mater.* **2018,** *30* (15), 5380-5389.
52. Tang, K.; Miao, W.; Guo, S., Crosslinked PEDOT: PSS Organic Electrochemical Transistors on Interdigitated Electrodes with Improved Stability. *ACS Appl. Polym. Mater.* **2021,** *3* (3), 1436-1444.
53. Gao, Y.-S.; Xu, J.-K.; Lu, L.-M.; Wu, L.-P.; Zhang, K.-X.; Nie, T.; Zhu, X.-F.; Wu, Y., Overoxidized polypyrrole/graphene nanocomposite with good electrochemical performance

as novel electrode material for the detection of adenine and guanine. *Biosens. Bioelectron.* **2014,** *62*, 261-267.
54. Li, Y.; Qian, R., Electrochemical overoxidation of conducting polypyrrole nitrate film in aqueous solutions. *Electrochim. Acta* **2000,** *45* (11), 1727-1731.
55. Si, P.; Chen, H.; Kannan, P.; Kim, D.-H., Selective and sensitive determination of dopamine by composites of polypyrrole and graphene modified electrodes. *Analyst* **2011,** *136* (24), 5134-5138.
56. Kato, H.; Nishikawa, O.; Matsui, T.; Honma, S.; Kokado, H., Fourier transform infrared spectroscopy study of conducting polymer polypyrrole: higher order structure of electrochemically-synthesized film. *J. Phys. Chem.* **1991,** *95* (15), 6014-6016.
57. Rivnay, J.; Leleux, P.; Sessolo, M.; Khodagholy, D.; Hervé, T.; Fiocchi, M.; Malliaras, G. G., Organic electrochemical transistors with maximum transconductance at zero gate bias. *Adv. Mater.* **2013,** *25* (48), 7010-7014.
58. Kaphle, V.; Liu, S.; Keum, C. M.; Lüssem, B., Organic electrochemical transistors based on room temperature ionic liquids: performance and stability. *Phys. Status Solidi A* **2018,** *215* (24), 1800631.
59. Cicoira, F.; Sessolo, M.; Yaghmazadeh, O.; DeFranco, J. A.; Yang, S. Y.; Malliaras, G. G., Influence of device geometry on sensor characteristics of planar organic electrochemical transistors. *Adv. Mater.* **2010,** *22* (9), 1012-1016.